

# Galaxy groups and haloes in the SDSS-DR7

Juan C. Muñoz-Cuartas<sup>1</sup>; Volker Müller<sup>1</sup>

<sup>1</sup> *Leibniz-Institut Für Astrophysik Potsdam, An der Sternwarte 16, 14482 Potsdam, Germany.*

Accepted XXXX December XX. Received XXXX December XX; in original form 2009 June 27

## ABSTRACT

In this work we introduce a new method to perform the identification of groups of galaxies and present results of the identification of galaxy groups in the Seventh Data Release of the Sloan Digital Sky Survey (SDSS-DR7). Our methodology follows an approach that resembles the standard friends-of-friends (FoF) method. However, it uses assumptions on the mass of the dark matter halo hosting a group of galaxies to link galaxies in the group using a local linking length. Our method does not assume any ad-hoc parameter for the identification of groups, nor a linking length or a density threshold. This parameter-free nature of the method, and the robustness of its results, are the most important points of our work. We describe the data used for our study and give details of the implementation of the method. We obtain galaxy groups and halo catalogs for four volume limited samples whose properties are in good agreement with previous works. They reproduce the expected stellar mass functions and follow the expected stellar-halo mass relation. We found that most of the stellar content in groups of galaxies comes from objects with  $M_r$  absolute magnitudes larger than -19, meaning that it is important to resolve the low luminosity components of groups of galaxies to acquire detailed information about their properties.

**Key words:** galaxies: haloes, groups – cosmology: dark matter, observations

## 1 INTRODUCTION

It is well known that on small scales galaxies are distributed in an inhomogeneous way. It is common to observe galaxies to be clustered, forming groups and clusters of galaxies. Nowadays it is understood, that the tendency of galaxies to cluster is a natural process associated with their formation and evolution.

Galaxies are thought to form from the gas that cools in the potential well of dark matter haloes. Posterior mergers between haloes induce the growth of dark matter structures and influence the process of galaxy evolution. Then, observing the spatial distribution of galaxies allows for an indirect investigation of the spatial distribution of the host dark matter haloes. Specifically, identification of galaxy groups allows the identification of the dark matter structures that host each group of galaxies.

Theoretically, dark matter haloes are associated with overdensities in the dark matter density field and galaxies hosted in these haloes may follow the local density enhancement. Then, from the observational point of view, since dark matter can not be observed directly, the overdensities in the mass density field have to be inferred from enhancements in the local number density of galaxies. Unfortunately there is not a general way to identify such enhancements, since galaxies are a biased tracer of the mass density field and it

is difficult to establish a density threshold or a border that marks the end of the distribution of galaxies that are associated to the same dark matter halo. The situation becomes even more complex when one considers the observational constraints on the data sets, like incompleteness due to the non detection of faint galaxies, or difficulties to resolve close pairs. Another difficulty comes from the fact that observationally we can not determine the positions of galaxies in real space. Because in galaxy surveys what we use to determine the distance to a galaxy is its redshift, and it encapsulates not only the effects of cosmic expansion but also information about the dynamics of the local neighbourhood in which the galaxy resides, the spatial distribution of the observational data must be interpreted as in redshift space instead of real space. All these inconvenients require the development of special techniques that allow the identification of galaxy groups.

Now, because the distribution of galaxies can be considered as a point process, the most straight forward way to identify groups of galaxies in a survey is to use the FoF method. In this method the clusters are identified using a percolation technique in which points are linked in clusters if their mutual and transitive distances are smaller than  $b$  times the mean interparticle distance. In numerical simulations, where the particles of the point process represent mass elements with a well known mass, one can choose the

value of  $b$  in order to select regions that are bounded by some given overdensity threshold. In observations, since the point process represents galaxies, and for instance there is no simple way to assign masses to each galaxy, the selection of the value of the linking length has to be done on an empirical basis, and only after tests one can choose a value that gives confident results (Berlind et al. 2006). Furthermore, in redshift space, due to the break in the spatial symmetry introduced by the redshift space distortions, one has to split the search in two orthogonal directions and then use two different linking lengths whose values have to be tuned upon the performance of tests.

In no way the identification of groups of galaxies as described above is a warranty of genuine group selection, and in the basic picture, it is not possible to obtain further information about their dark matter haloes.

Previously, exploiting the wealth of data provided by the already existing surveys, many works have focused on the identification of groups of galaxies in galaxy redshift surveys. For instance, Berlind et al. (2006) have performed the identification of groups of galaxies in the third data release of the Sloan Digital Sky Survey. Besides the groups of galaxies and their properties, they have shown in their work a detailed study on the effects of the selection of the linking length, finding an optimal value that allows them to study halo occupation statistics. Later Crook et al. (2007), using a percolation method, presented the identification of groups of galaxies in the Two Micron All Sky Redshift Survey (2MASS). Their samples have been designed to maximize the number of rich groups and those required to be identified above some given overdensity threshold. They also present a match between the most massive groups in their catalog with previously well known groups and clusters of galaxies.

Merchán & Zandivarez (2005) have proposed a standard implementation of the FoF method in flux limited samples. In their implementation they avoid artificial merging of small groups and perform an improved determination of the group center for rich groups. They implemented the method on the third data release of the SDSS. Zapata et al. (2009) and Zandivarez & Martínez (2011) also have used this prescription to perform the identification of groups in different releases of the SDSS. Particularly, Zandivarez & Martínez (2011) have used this prescription to identify groups of galaxies with at least four members. They have used linking lengths that correspond to overdensities comparable to those used to define dark matter overdensities in standard  $\Lambda$ CDM cosmology and computed the virial halo mass from an estimated virial radius and the velocity dispersion of member galaxies.

Koester et al. (2007) have used the MaxBCG method to identify clusters of galaxies in the SDSS. The method, based on the likelihood associated to a galaxy to be a BGC and a likelihood associated to the spatial, morphological and photometric properties of the galaxy, uses a percolation algorithm to identify groups. Particularly, they show a high purity of the clusters they identify with this method. Geach et al. (2011) have used a technique based on a Delaunay tessellation on sets of galaxies distributed by colour. With this method, they identify photometrically selected clusters of galaxies out to a redshift  $z \sim 0.6$ . Although this method allows the identification of potential clusters at high red-

shift, it is difficult to actually confirm the physical relation among cluster members. Lee et al. (2004), Nichol (2004), Wen et al. (2009), Tago et al. (2008) and Tago et al. (2010), have also shown the identification of groups of galaxies in different data releases of the Sloan Digital Sky Survey.

Of particular interest for our work has been the group catalog presented in Yang et al. (2007) (hereafter YHC). In YHC, on top of a standard FoF group identification, they perform a halo based identification of groups of galaxies hosted in the same dark matter halo. Several different studies have shown the good performance of such a group finder. Their halo catalog, which is based on the data of the Fourth Data Release of the SDSS, has been used in different works to study the conditional luminosity function (Yang et al. 2005a, Yang et al. 2005b, Wang et al. 2008), environmental properties of galaxies (Wang et al. 2011, Wetzel et al. 2011, Weinmann et al. 2011 and Wang et al. 2008), the distribution of dark matter on large scales (Muñoz-Cuarteras et al. 2011), among others. Recently Tinker et al. (2011) have used the same method to identify the groups of galaxies in the SDSS-DR7 to study the galaxy-halo connection.

In this work we revisit the problem of the identification of groups of galaxies in galaxy redshift surveys, and the identification of dark matter haloes from the groups of galaxies they host. Our method is inspired by the method of Yang et al. (2007), and follow the ideas of hierarchical growth of structures for the assembly of dark matter haloes as well as the ideas of the standard FoF method.

We assume that each galaxy has an associated dark matter halo, with a mass that depends on the luminosity or the stellar mass of the galaxy it hosts. Then we use the estimated halo mass to compute its properties, and make the search of neighbouring galaxies in an ellipsoidal region, with axes determined by the virial radius of the halo and its maximum circular velocity. In this way, we merge groups that intercept the ellipsoid of a given halo, in a similar way as the FoF method, with the difference that the linking length is local and completely dependent on the properties of the dark matter halo that is being the current center of search.

Our procedure provides two major improvements on previous percolation methods. First, the linking lengths for search of neighbouring galaxies is local, and it depends only on the properties of the halo that is the center of search. And second, and more important, no assumption about the value of the initial linking length or any other parameter has to be made for the identification of galaxy groups and haloes. Therefore our method is parameter free. Furthermore, like the method of Yang et al. (2007), the identification of groups of galaxies leads directly to the identification of dark matter haloes in the survey with reliable mass estimates. On the other hand, our method differs from that presented in Yang et al. (2007) in several aspects. First, we do not need to make an initial FoF procedure in redshift space to start the iterations of the groups. This avoids possible contamination by the choice of the initial linking lengths. Second, differently from the assumption made in Yang et al. (2007), we do not need to assume an initial value for the mass-to-light relation of groups. And third, our method uses a two dimensional spheroid for the search of group members, much in the way as the FoF algorithm with two orthogonal adaptive linking lengths. This is different from the implementation in Yang et al. (2007), where they use a fixed FoF linking length for

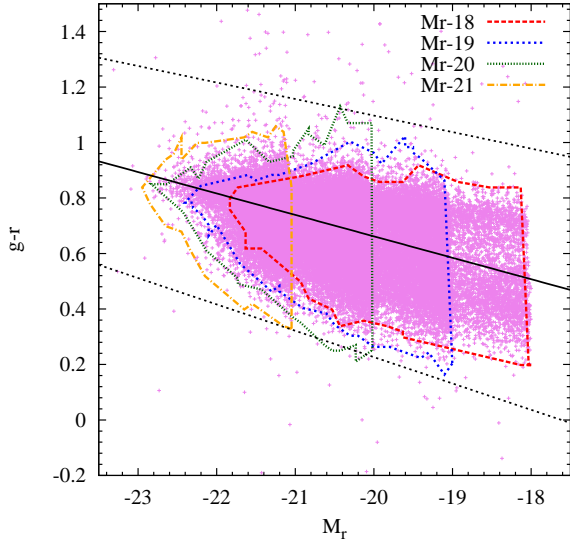


**Figure 1.** Colour magnitude diagram for the galaxies in the four volume limited samples. The straight lines represent the mean and  $3\sigma$  levels used to adjust the colour used in the estimation of the stellar mass  $M_*$  for those colour outliers. The contours indicate the regions in the diagram delimited by each galaxy sample.

the transverse search and a probabilistic approach for the redshift distribution of galaxies, that at the end requires the use of another free parameter to fix the density contrast defining the membership of galaxies in groups.

In what follows, in Section 2 we introduce the method for identification of groups of galaxies. Then in section 3 we present the data set used to implement the method presented in the work. Then in section 4 we present the results of the implementation of our method on the data of the Seventh Data Release of the SDSS. Finally we summarise and discuss our results.

## 2 GROUP IDENTIFICATION METHOD

Our group finder is based on the idea of haloes, and is inspired in the philosophy of a standard FoF group finder as well as from the group finding method proposed by Yang et al. (2007).

In the standard FoF method, one usually chooses a fixed linking length that is a fraction  $b$  of the mean inter-particle distance. Particles that are closer than this linking length are labelled as members of the same cluster, where the membership is transitive through all particles in the data set, this means that through the particle distribution, *friends of my friends are also my friends*. In N-body simulations one can show that using a linking length  $b = 0.2$  times the mean interparticle separation, the overdensity of the structures identified is around 170 times the mean density of the universe, a number that is in close agreement with the expectation from spherical collapse model for virialized structures. Also, because of the isotropy of the particle distribution, only one linking length is required for the search in the 3D space.

In the case of observational data points the search has to be split in a two dimensional problem because the redshift

space distortions breaks the spatial symmetry of the distribution of points (galaxies). Then it is required to make the search in two orthogonal directions using two different linking lengths. In this case the selection of both linking lengths becomes arbitrary. First, because now the data points do not represent mass elements, but galaxies, for which we do not know a-priori the amount of mass they represent, i.e. one can not use the same arguments as in simulations to determine the value of the linking lengths. Second, the amount of distortion introduced by redshift space effects is unknown, and it depends on different factors like the host halo mass, the mass of the satellite galaxy, and their positions relative to the observer. In this case, to obtain reliable results on the identification of groups, one has to look for the set of parameters that gives the best results according to the expected properties of the clusters (Bell et al. 2006, Tago et al. 2005, Tago et al. 2010).

We aim to perform the search of groups of galaxies residing in the same dark matter halo. Our approach uses a local linking length criteria, that depends only on the properties of the assumed host dark matter halo associated with every galaxy group. Now we describe our method step by step.

### Initialization:

Before start, we have to prepare a set of quantities for each galaxy in the galaxy catalog. We compute the galaxy's stellar mass, luminosity in the  $r$  band, comoving Cartesian coordinates and estimate the halo mass and radius.

We first compute for each galaxy its stellar mass  $M_*$ . Following Yang et al. (2007) we do so through

$$\log(M_*) = -0.306 + 1.097(g-r)^0 - \epsilon + \log(L_r) \quad (1)$$

where we have used the relations from Bell et al. (2003) to estimate the stellar mass from the mass to light ratios.  $(g-r)^0$  is the colour of the galaxy corrected to  $z=0$ ,  $\epsilon$  is a parameter that depends on the initial mass function, that in our case is  $\epsilon = 0.15$  (Bell et al. 2003), and  $L_r$  is the luminosity of the galaxy in the  $r$  band, that has been computed as

$$L_r = 10^{0.4(M_{\odot,r} - M_r)} \quad (2)$$

with  $M_{\odot,r} = 4.76$  (Blanton & Roweis 2007). As discussed in Yang et al. (2007), some galaxies in the catalog are outliers of the colour magnitude diagram. Using these values for the colours in eq. 1 will produce unreliable stellar masses for these galaxies. We do not know the reason of the exceptional behaviour of these galaxies, and therefore it is not clear how to assign a colour to them. For this reason we assume the simplest approach. For galaxies that are  $3\sigma$  values off from the mean value of  $(g-r)^0$  in the colour magnitude diagram, we estimate their stellar masses using the mean value for the colours of the galaxies with the same  $L_r$  luminosity. Figure 1 shows the colour magnitude diagram for our four volume limited samples as well as the mean and  $3\sigma$  levels. As it can be seen, only a small fraction of the galaxies in the sample need their stellar masses to be corrected for colour.

For every galaxy we compute also their comoving Cartesian coordinates from

$$x_i = r_i \cos(\delta_i) \cos(\alpha_i),$$

$$\begin{aligned} y_i &= r_i \cos(\delta_i) \sin(\alpha_i), \\ z_i &= r_i \sin(\delta_i), \end{aligned} \quad (3)$$

where  $\alpha_i$  and  $\delta_i$  are the right ascension and declination of each galaxy in the catalog and  $r_i$  is the comoving distance of the respective galaxy, given by

$$r_i = c \int_0^{z_i} \frac{dz}{H_0 \sqrt{\Omega_m(1+z)^3 + \Omega_\Lambda}}, \quad (4)$$

with  $c$  being the speed of light,  $\Omega_m = 0.258$  is the mass density parameter and  $H_0 = 72 \text{ km s}^{-1} \text{ Mpc}^{-1}$  is the Hubble constant at present time.

Then, we assume that every galaxy resides in a dark matter halo of a given mass. We assign mass to the dark matter halo of each galaxy relating the stellar mass (or the  $L_r$  luminosity) of the galaxy with the mass of dark matter haloes sampled from a theoretical mass function (Warren et al. 2006, Sheth & Tormen 2002) between mass limits  $M_{min}$  and  $M_{max}$ . Later we will describe how we define these limiting values.

Once each halo has a mass, we compute their radius assuming they satisfy virialization criteria. Then each halo has a radius  $R_{vir}$  given by

$$R_{vir} = \left( \frac{3M_{vir}}{4\pi\Delta_{vir}\rho_{crit}} \right)^{1/3}. \quad (5)$$

We have assumed that the mass assigned to the halo coincides with its virial mass, and use the mean overdensity of haloes in the spherical collapse  $\Delta_{vir}$  relative to the critical density of the Universe,  $\rho_{crit}$ , evaluated at  $z = 0.1$  (Bryan & Norman 1998). After this, we sort the halo catalog in decreasing order of mass to start iterations from the most massive haloes to the low mass ones. In this initial situation each halo hosts one galaxy. We set the position of the halo to coincide with the position of the galaxy it hosts.

#### Iteration:

*Step one:* Once there is an initial halo catalog (haloes with positions, radius and masses) we can start linking haloes that are close to each other. Starting from the most massive halo ( $S_h$ ) we search for the haloes ( $S_i$ ) that are contained in a sphere of radius  $R_{zs}$  centred at the position of halo  $S_h$ . The radius of the sphere  $R_{zs}$  is given by

$$R_{zs} = \frac{V_{max}}{100} [h^{-1} \text{ Mpc}] \quad (6)$$

where  $V_{max}$  is in units of  $\text{km s}^{-1}$  and represents the median maximum circular velocity of the halo  $S_h$  with mass  $M_{vir}$  that is center of search.  $V_{max}$  is approximated by

$$V_{max} = 0.0325 \left( \frac{M_{vir}}{M_\odot} \right)^{0.31} [\text{km s}^{-1}] \quad (7)$$

as computed from high resolution cosmological simulations (Muñoz-Cuertas et al. in prep.). Instead, we could have used the halo velocity dispersion  $\sigma_v$ , which would have been more appropriate from the theoretical point of view. However we tested both approximations and the differences are small since both quantities are comparable. On the other hand, using  $V_{max}$  produces a region of search  $R_{zs}$  that is slightly larger than the one using  $\sigma_v$ . We prefer a larger  $R_{zs}$  to

maximize the number of members per group with the hope that using a large  $R_{zs}$  the effects of redshift space distortion are treated more carefully. Finally, tests against mock catalogs have shown that this choice produces the results with the highest purity and completeness, compared to  $\sigma_v$  or  $V_{vir}$ .

For the set of haloes  $S_i$  that are inside the sphere of search  $R_{zs}$  we perform a set of operations:

- (i) We evaluate their positions relative to the position of the halo  $S_h$
- (ii) Rotate the coordinates of the haloes in  $S_i$  to a system of coordinates such that the line of sight coincides with the  $z$ -axis.
- (iii) Search for the subset of haloes  $S_m$  in  $S_i$  that are contained in the spheroid defined by

$$f(R_{vir}, R_{zs}) = \frac{x^2}{R_{vir}^2} + \frac{y^2}{R_{vir}^2} + \frac{z^2}{R_{zs}^2}. \quad (8)$$

Here  $R_{vir}$  is the virial radius of the halo  $S_h$ .

Now the meaning of the quantity  $R_{zs}$  becomes clear.  $V_{max}$  represents the maximum circular velocity of a particle in the potential of the host halo  $S_h$ , then it sets a limit for the velocity of a galaxy moving inside the halo. If a galaxy moves with a peculiar velocity  $V_{max}$  along the line of sight, then its observed velocity will be  $V_{obs} = V_{max} + V_H$  where  $V_H$  is the Hubble flow at the position of the halo  $S_h$ . Then, if we approximate the distance to the galaxy as  $d = (V_{max} + V_H)/H_0$  it becomes clear that  $R_{zs}$  will represent the maximum distance along the line of sight from the center of the halo  $S_h$  at which we can find a galaxy bound to its potential well.

Note that the use of an ellipsoidal window function accounts for the projection effects of the peculiar velocities, which are maximum along the line of sight, but reduce gradually out of this line. Particularly, note that galaxies (and haloes) with no projected velocities along the line of sight, but at a distance  $R_{vir}$  from the center of the halo (galaxies moving perpendicular to the line of sight) will be included as members of the group. This process tries to recover the spatial symmetry of the point process that is broken by the redshift space distortions. It also avoids the ad-hoc splitting of the search in to two orthogonal directions with two different linking lengths with no physical relation between them.

*Step two:* All haloes in the subset  $S_m$  that fall inside the spheroid delimited by  $f(R_{vir}, R_{zs})$  are merged with the halo  $S_h$ . In this process, all galaxies inside the small haloes in  $S_m$  will be incorporated in the halo  $S_h$ . The position of the resulting halo will be relocated to the position of the galaxy with the largest stellar mass. The final mass of the halo right after merging will be the sum of the masses of the haloes that merged.

Total stellar masses in groups are then computed as the sum of the stellar mass of the individual galaxies  $M_{*,i}$  weighted by their completeness  $c_i$

$$M_{stellar} = \sum_i \frac{M_{*,i}}{c_i} \quad (9)$$

Similarly, characteristic luminosities in the  $r$  band,  $L_{ch}$ , of each group are computed from the luminosity of their galaxy members as

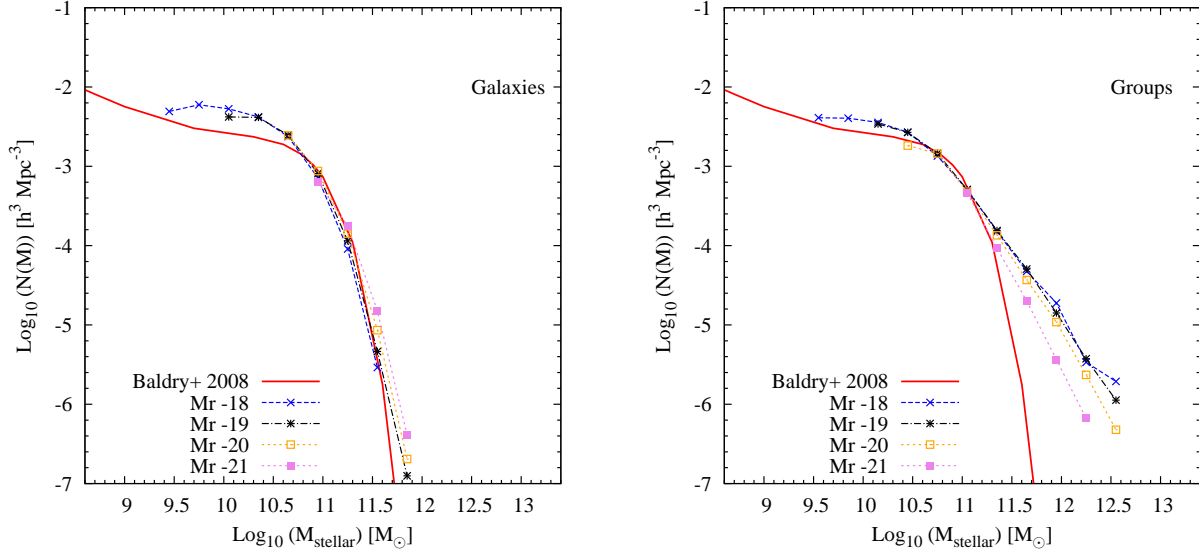


**Figure 2.** Stellar mass functions for galaxies and groups for our four volume limited samples. The solid line shows the stellar mass function of Baldry et al. (2008).

$$L_{ch,g} = \sum_i \frac{L_{r,i}}{c_i} \quad (10)$$

As discussed in Yang et al. (2007), weighting the stellar mass and luminosity with the completeness accounts for the missing objects in the same region of the survey.

Haloes that are already merged in larger haloes are removed from the halo catalog for the next iteration. Then, during the procedure, the halo population changes but not the galaxy population.

*Step three:* After applying this procedure to all haloes  $S_h$ , in decreasing order of mass, and considering that the population of haloes will change each time small haloes merge with the big ones, we end up with a new distribution of galaxies in haloes and a new halo catalog. We then update the halo list and sort the halo catalog in decreasing order of mass.

*Step four:* Once the halo catalog is sorted, we assign masses to haloes. We assume a one-to-one correspondence between halo mass and group stellar mass or group characteristic luminosity  $L_{ch}$ . Using the estimated comoving volume of the sample of galaxies, we compute a minimum  $M_{min}$  and a maximum mass  $M_{lim}$  necessary to host all haloes in the halo catalog. The mass limits are obtained from the mass function solving the equations  $N(> M_{lim}) = 1$  and  $N(> M_{min}) = N_h$ , where  $N(> M)$  is the cumulative mass function representing the number of haloes with mass larger than  $M$  and  $N_h$  is the number of haloes in the halo catalog at a given iteration.

Because during the first iterations (for the initialization step, and a few initial iterations) we associate mostly individual galaxies with individual haloes, the use of the limit halo mass  $M_{lim}$  will associate unreliable massive haloes to individual galaxies, for example, galaxies with a stellar mass of  $\sim 10^{12} h^{-1} M_\odot$  could be associated with a halo with a mass of  $> 10^{14} h^{-1} M_\odot$ . This high mass will lead to large

linking lengths  $R_{vir}$  and  $R_{zs}$  to these haloes, i.e, the massive haloes would grow very rapidly and would hinder the identification of smaller haloes. This would have a negative effects on the final distribution of groups and haloes. To avoid it we fix, for each iteration, an ad-hoc maximum halo mass  $M_{max} < M_{lim}$  and sample randomly  $N_h$  halo masses from the mass function in the range of masses  $[M_{min}, M_{max}]$ . Then we iteratively shift the value of  $M_{max}$  by some amount  $dM$  until it reaches the maximum allowed halo mass in the volume,  $M_{lim}$ . In this way we do a physically reasonable mass assignment to massive groups in each iteration, and control the growth of the linking lengths of haloes.

Then, we generate  $N_h$  halo masses sampling the mass function in the interval  $[M_{min}, M_{max}]$ . Then, halo masses are assigned, in each iteration, relating them to the galaxy groups according to the group stellar mass  $M_{stellar}$  or the group characteristic luminosity  $L_{ch}$ , in a way that the groups with the largest  $M_{stellar}$  or  $L_{ch}$  will be associated to the most massive halo mass.

*Iterate all steps:* We iterate the previous steps (one to four) for a given pair of values of  $M_{min}$  and  $M_{max}$  starting with  $M_{max} = 10^{12} h^{-1} M_\odot$ . Once this iteration converges to a fixed number of haloes, we increase the value of  $M_{max}$  by an amount  $dM = \Delta \log_{10}(M) = 0.5$ . Since the number of haloes in the population have changed, we recompute the value of  $M_{min}$ , and repeat the process from the first step with these new values of  $M_{min}$  and  $M_{max}$ . This process has to be repeated until  $M_{max} = M_{lim}$ .

We have found that a reasonable value for  $M_{max}$  to start the iteration is  $10^{12} h^{-1} M_\odot$ , which approximately corresponds to the mass of the halo of massive galaxies at  $z = 0$ . We have tested different values of the starting  $M_{max}$  and  $dM$  and found no differences in the final population of groups. In conclusion our results are weakly dependent on the choice of  $M_{max}$  and  $dM$ . The independence of the final results on  $M_{max}$  and  $dM$  is due to the double-iteration process that controls the evolution of the population of haloes.

Note that our method does not assume any ad-hoc parameter for the identification of groups, nor a linking length or a density threshold. The parameter-free nature of the method, and the robustness of its results are one of the most important points of our work.

### 3 THE DATA SAMPLE

Our galaxy groups are identified from the SDSS Seventh Data Release (Abazajian et al. 2009). We use data for the SDSS-DR7 publicly available from the VAGC (Blanton et al. 2005). The data release from the VAGC has improvements on the photometric reductions, calibration as well as deals with the problems associated with multiple observations of the same object. To produce our fiducial galaxy catalog from the VAGC catalog we first select objects that are targeted simultaneously as “GALAXY” and have been targeted in the spectroscopic survey. Furthermore we request the object to belong to the main galaxy sample (“VAGC\_SELECT=7”) and to be a well resolved spectral target (“RESOLVE\_STATUS&256”). Our initial galaxy sample extends from  $z = 0.002$  to  $z = 0.2$ . For all galaxies in this sample we compute the  $K$ -corrected absolute magnitudes using the KCORRECT code (V4.2, Blanton et al. 2007). Absolute magnitudes are computed as shown in Yang et al. (2007), from

$$M_x - 5 \log h = m_x - DM(z) - K(z) - A_x(z - z_n) \quad (11)$$

where the subscript “ $x$ ” stands for the different magnitude band  $x = (u, g, r, i, z)$ ,  $M_x$  is the absolute magnitude of the galaxy,  $m_x$  is the apparent magnitude of the galaxy as given in the catalog,  $DM(z)$  is the distance modulus,  $K(z)$  is the  $K$ -correction term and  $z_n = 0.1$  is the reference redshift. The coefficients  $A_x$  quantify the correction for evolution, and are taken from Blanton et al. (2003) to be  $A_x = (-4.22, -2.04, -1.62, -1.61, -0.76)$  for the five colours.

Following Tago et al. (2010), we generate four different volume limited samples, taken from the previously described galaxy sample, each with magnitude cut  $M_r = -18, -19, -20$  and  $-21$ . The redshift limits are  $z_{min} = 0.002$  and  $z_{max} = 0.047, 0.074, 0.115$  and  $0.175$  respectively. We have imposed a limit at  $M_r = -23.5$  as the maximum absolute magnitude of a galaxy in the sample. No more than ten galaxies are discarded at this step. Table 1 summarizes the properties of the four volume limited samples used in this work. The total comoving volume occupied by each galaxy sample is estimated using a Delaunay tessellation, which allows us to estimate the volume of each galaxy, and then the total volume as the sum of the volumes of all galaxies in the sample<sup>1</sup>.

## 4 RESULTS

Tables 2 and 3 summarize the results of the group finder applied to the four volume limited samples built from the

Name	$z_{min}$	$z_{max}$	$N_{gals}$	$L_{eq} h^{-1} \text{ Mpc}$
Mr-18	0.002	0.047	50986	130
Mr-19	0.002	0.074	108546	200
Mr-20	0.002	0.115	155890	310
Mr-21	0.002	0.175	97064	465
All	0.002	0.2	412486	

**Table 1.** Summary of the properties of the volume limited samples used for the construction of the groups of galaxies in the survey.  $L_{eq}$  represents an estimate of the size of the equivalent cubic comoving box with the same volume as the sample of galaxies.

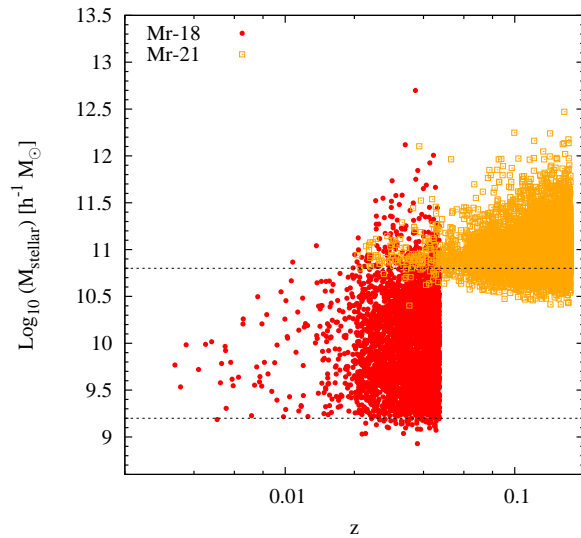


**Figure 3.** Group stellar masses as a function of redshift for the groups identified in two of the four samples. The horizontal lines indicate approximate masses where the set of haloes will be complete in stellar mass.

SDSS-DR7. There, richness, halo mass, stellar mass and luminosity limits (minimum and maximum values per sample of galaxies) are shown.

In the next sections we study in detail the stellar mass content, halo masses, luminosities and the richness of the groups identified in the data with the implementation of the method presented in the previous section.

### 4.1 Stellar mass

As a first check, we verify that the stellar mass assignment in galaxies produces reasonable results. Figure 2 shows the stellar mass function for galaxies and groups for our four volume limited samples. Note that our data only goes until  $\sim 10^{9.5} h^{-1} M_\odot$  due to the high magnitude cut imposed to build the volume limited samples. To make this comparison we have estimated the mass function as the number density of galaxies with stellar mass  $M$  in the range between  $M$  and  $M + dM$ , where the stellar mass is the result of the estimate from eqs. 1 and 9 weighted by the completeness of the survey at the position of the galaxy, all divided by the total volume of the sample of galaxies.

<sup>1</sup> We have used the publicly available code Qhull (Bradford et al. 1996) to compute the Delaunay tessellation.

Name	$N_h$	$\log_{10}(M_{min})$	$\log_{10}(M_{lim})$	$N_{gr}(N = 1)$	$N_{gr}(N = 2)$	$N_{gr}(N = 3)$	$N_{gr}(N \geq 4)$
Mr-18	38268	11.2	14.7	33863	2746	691	968
Mr-19	85222	11.5	14.9	76220	5568	1495	1939
Mr-20	128975	11.9	15.1	116620	7878	2077	2400
Mr-21	87040	12.7	15.2	80881	4344	996	819

**Table 2.** Table summarizing the properties of the groups for the four different samples.  $N_h$  shows the final number of haloes in the sample.  $M_{min}$  and  $M_{max}$  are the minimum and maximum halo mass in the sample in units of  $h^{-1} M_\odot$  and  $N_{gr}(N = 1)$ ,  $N_{gr}(N = 2)$ ,  $N_{gr}(N = 3)$  and  $N_{gr}(N \geq 4)$  show the number of groups with one, two, three and more than four members.

Name	$N_h$	$\log_{10}(M_{stellar}^{min})$	$\log_{10}(M_{stellar}^{lim})$	$\log_{10}(L_{ch}^{min})$	$\log_{10}(L_{ch}^{max})$	$R_{zs}^{min}$	$R_{zs}^{max}$
Mr-18	38268	8.9	12.7	9.1	12.2	0.9	11.6
Mr-19	85222	9.4	12.6	9.5	12.1	1.1	14.1
Mr-20	128975	9.8	12.7	9.9	12.1	1.6	15.2
Mr-21	87040	10.3	12.5	10.3	11.8	2.7	17.3

**Table 3.** Table summarizing the properties of the groups for the four different samples.  $M_{stellar}^{min}$  and  $M_{stellar}^{lim}$  show the maximum and minimum group stellar mass in each sample in units of  $h^{-1} M_\odot$ .  $L_{ch}^{min}$  and  $L_{ch}^{max}$  are the minimum and maximum group characteristic luminosity in units of  $h^{-1} L_\odot$  and  $R_{zs}^{min}$  and  $R_{zs}^{max}$  are the minimum and maximum ellipsoidal radius of search along the line of sight in  $h^{-1} \text{Mpc}$ .

For galaxies, our stellar mass function follows closely the mass function presented in Baldry et al. (2008) in the range of masses between  $\sim 10^{9.5}$  and  $\sim 10^{11.5} h^{-1} M_\odot$ . We can also see in Figure 2 that for masses below  $\sim 10^{11.5} h^{-1} M_\odot$  the stellar mass function for groups have roughly the same behaviour as the stellar mass function for individual galaxies. For masses larger than  $10^{11.5}$  the abundance of stellar-massive objects is larger, but it is almost the same for the three samples with the lower luminosity cuts. As expected, the number density of groups with a given stellar mass is lower for the sample associated with the high luminosity cut. This behaviour implies that the contribution from galaxies with absolute magnitudes below  $M_r = -20$  to the stellar mass is important in characterizing the baryonic content of massive groups. Also, as will be seen later in the analysis of the richness, the groups with stellar masses below  $\sim 10^{11.5} h^{-1} M_\odot$  are associated to groups with less than  $\sim 10$  members. This low number of members, and therefore, low total stellar mass, is responsible for the agreement between the stellar mass function of individual galaxies and groups at low masses.

Since we assign masses to groups using the ranking of luminosities, because for construction the samples are complete in luminosity, the group stellar masses are not necessarily complete in each volume limited sample. That is shown in Figure 3, where we show the distribution of stellar masses for groups as a function of redshift. The only sample that is almost complete in stellar mass is Mr-18, the other three samples are incomplete due to the lack of contributions to the stellar mass from the low mass galaxies not included in each sample.

Figure 4 shows the stellar mass as a function of halo mass for the four samples. For comparison we also plot the results from the halo catalog of Yang et al. (2007) and the fitting formula from Moster et al. (2010). Halo masses have been computed through the ranking of the group stellar

masses. Note however that this mass assignment is technically incorrect if one uses samples that are not complete in stellar mass. We have made comparisons between the mass assignment using complete samples in stellar mass and our final incomplete samples, and since the incompleteness affects a small fraction of groups at the low mass end, the average results are comparable. However, we will not assume this halo mass to be a final reliable quantity. We keep it for completeness and to help us to evaluate the performance of the halo mass assignment.

Here we see again the effect of the underestimation of the stellar mass for the groups in the high luminosity sample, which in this case leads to the underestimation of the stellar masses of groups hosted in haloes with high masses. The small tails seen at the low halo mass end are associated with the incompleteness of the samples in stellar mass shown in Figure 3. We have tested it, and complete samples in stellar mass do not present such a tails. From this figure we can see, first, that there is agreement between the stellar and halo mass among our four volume limited samples, as well as with the halo catalog from Yang et al. (2007). Second, we see that our samples also follow the expected stellar-halo mass relation from Moster et al. (2010) up to  $\sim 10^{13.4} h^{-1} M_\odot$ , where both, our catalogs, and the one from Yang et al. (2007) show an upturn in the observed stellar mass. This upturn seems to be associated to the stellar mass of groups, not for individual star forming objects, as is assumed in Moster et al. (2010).

Figure 5 shows the stellar-halo mass relation for groups and central galaxies. For these plots the halo masses have been computed using the ranking on the group characteristic luminosities. From those figures we see the origin of the upturn in the stellar-halo mass relation for haloes more massive than  $\sim 10^{13.4} h^{-1} M_\odot$ . In figure 5 (left) we show the stellar-halo mass relation, for the stellar mass of the central galaxy in the group. Figure 5 (right) shows the same, but in



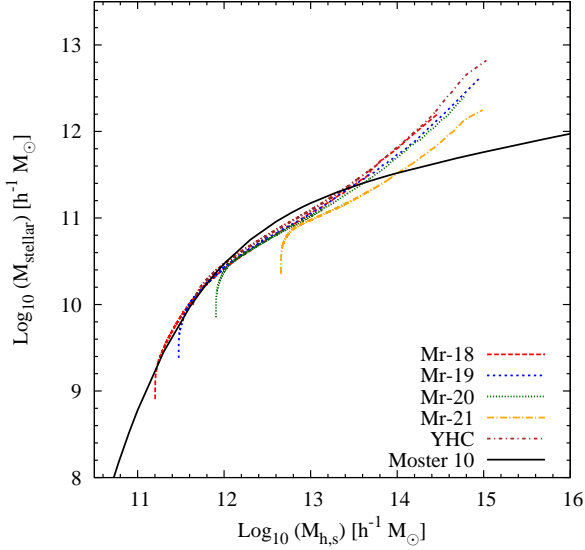


**Figure 4.** Stellar mass - halo mass relation for groups in the survey. Halo masses have been assigned using the ranking of group stellar mass. Filled-cyan points show the data from Yang et al. (2007) and the dashed line shows the prediction from Moster et al. (2010).

this case the stellar mass includes the contribution from all of the galaxies in the group. This confirms that the upturn in the stellar-halo mass relation comes from the contribution of group members in the stellar mass of the halo hosting it.

Note that for the sample Mr-21, the stellar-halo mass relation for groups (Figure 5, right) is different from the other three samples, while is the same for the stellar-halo mass relation for the central galaxies (Figure 5, left). This is the result of the low group richness in this sample due to the absence of low luminosity galaxies in Mr-21.

We can see also in Figure 5 (left) that the stellar-halo mass relation we obtain follows closely the predictions from Moster et al. (2010), but differences appears and increase for high halo masses. We see that at high halo masses our data underestimates the stellar mass compared to the prediction. It is difficult to find a reason for this discrepancy. If it were a problem with the assignment of stellar mass to galaxies (eq. 1), we should not be able to get the agreement with the stellar mass function. If it were a problem with the halo mass assignment, resulting from the estimation of  $M_{min}$  and  $M_{lim}$ , one would move our data points horizontally. That is, changing  $M_{min}$  and  $M_{lim}$  in the same amount by modifying the physical volume of the sample would solve the issue at the high mass end, but will introduce a stronger disagreement at the low mass end. Almost nothing will happen if we fix  $M_{min}$  and make  $M_{lim}$  smaller. Therefore we have no explanation for the differences.

#### 4.2 Characteristic luminosity

Due to the volume limited nature of the samples, one of the most important quantities for our catalog is the group luminosity. Figure 6 shows the group stellar mass as a function of the group luminosity. Again, each colour shows the results for each of the sample catalogs while the cyan points

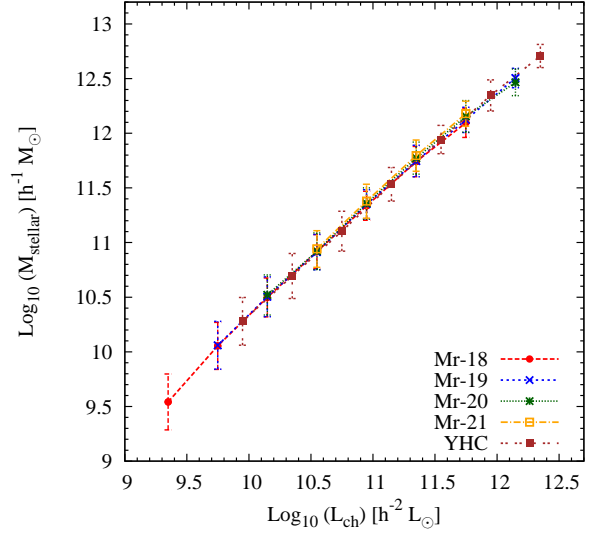


**Figure 6.** Median stellar mass as a function of the group luminosity. Error bars indicate dispersion on the data in each bin.

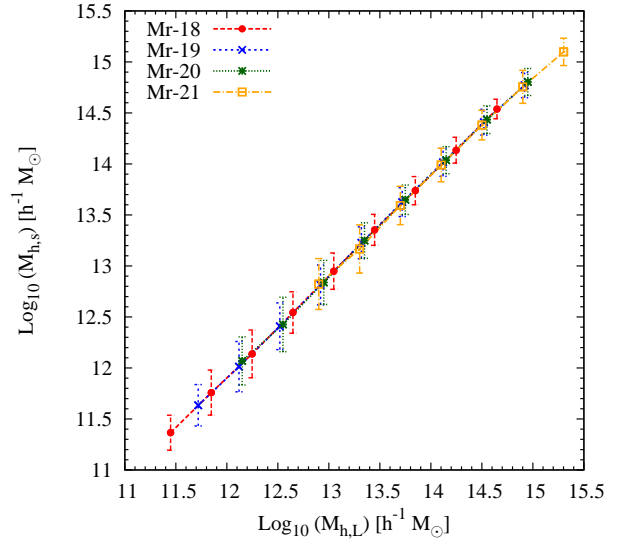


**Figure 7.** Median halo masses estimated using the ranking on the stellar masses as a function of the halo masses computed using the ranking of halo luminosities. Error bars indicate dispersion on the data in each bin.

shows the comparison with YHC. Note the scatter in stellar mass for a given halo luminosity. This is partly due to the procedure used in the estimation of the stellar masses of the galaxies in the galaxy sample, but must also be due to a component of intrinsic scatter associated to it. Clearly the scatter decreases as a function of group luminosity, and we can see here again the presence of a few groups with very massive stellar components, that seems to be in agreement also with the results shown in YHC.

As a comparison, Figure 7 shows the halo mass as computed from the ranking of the stellar masses ( $M_{h,s}$ ) as a function of the halo mass computed from the ranking of the



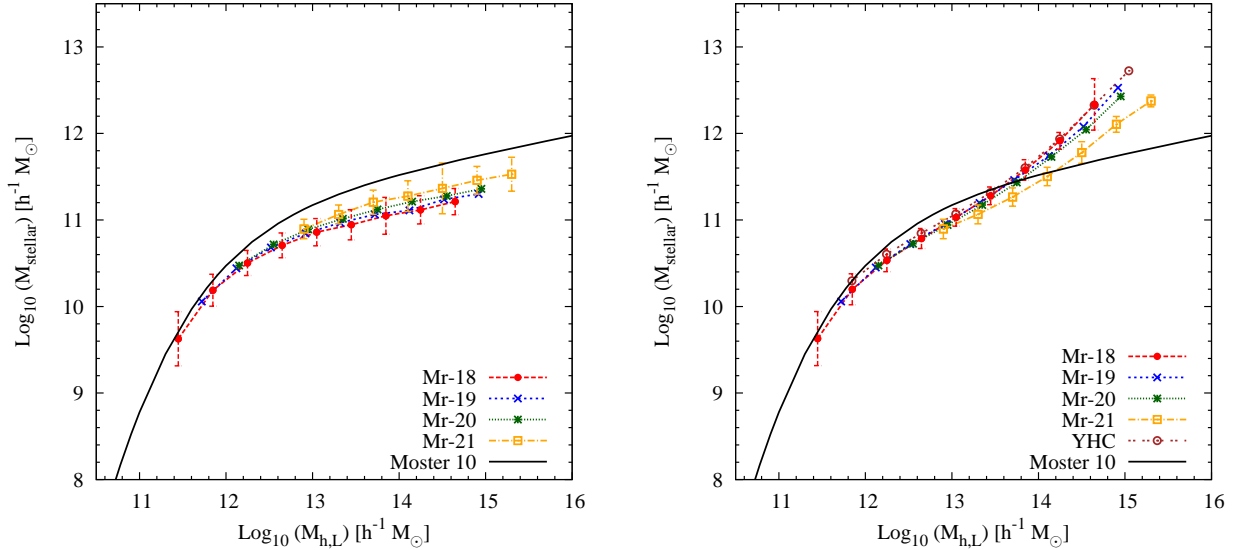


**Figure 5.** Median stellar mass of the central galaxy as a function of the halo mass. Halo masses are assigned using the ranking of the group characteristic luminosity. The frame at the left shows the relation using only the stellar mass in the central galaxy of the group while the frame at the right shows the the full stellar content in the group of galaxies computed from eq. 9. Error bars indicate dispersion on the data in each bin.

group luminosities ( $M_{h,L}$ ). Note first that there is a scatter in the estimation of the masses for both methods, and the scatter increases (for the same sample) at low halo masses. Although there is a natural scatter in the distribution of stellar masses at a given characteristic luminosity, this effect at low halo masses is partly a consequence of the incompleteness in stellar mass of the groups. This can be verified if one considers the small scatter for the sample Mr-18, which is the sample close to be complete in stellar mass. Interestingly, one can see that in the mean, both methods provide the same mass assignment, the slope of the relation is the same for all volume limited samples, which means that the estimated halo masses are robust. Note that this effect is independent on the incompleteness in stellar mass, and the already mentioned failure of the sample Mr-21 to reproduce the stellar mass function. That both methods produce, in the mean, the same halo mass is because the implementation of the method in volume limited samples that influences all groups by same amount. This means that in general, if there is an underestimation of stellar content in a group, all groups in the same sample are missing the same fraction of mass, and at the end, the more massive and luminous groups still are the most massive and luminous ones independent on the magnitude cut. In that way, the ranking and halo mass assignment is not affected by the absence of low mass-low luminosity galaxies in the samples with a high luminosity cut.

### 4.3 Richness

Figure 8 shows the mean comoving density of groups as a function of redshift (top left). The richness of groups as a function of group stellar mass (top right) and halo mass estimated using the two different approaches, the ranking of the halo luminosities (bottom left) and the ranking of the stellar masses (bottom right). The lines with symbols

in those plots show the mean richness as a function of mass computed in mass bins of 0.3dex.

The mean density is computed as described in Muñoz-Cuartas et al. (2011). Using a Delaunay tessellation we compute the mean number density of groups as a function of distance from the observer. As it can be seen in Figure 8, the mean number density of groups is almost constant for all samples. Again, the different normalization is due to the different abundance of groups identified in the different galaxy samples due to the different luminosity cuts. The thick lines in figure 8 shows the mean number density estimated using radial bins of  $14h^{-1}$  Mpc width while the thin lines show the same computed in radial bins of  $10h^{-1}$  Mpc.

We can see in Figure 8 that in all samples, the groups with the largest stellar mass and the largest halo mass are the richer ones. We can see in particular, that the group with the largest stellar mass is resolved by many galaxies in the low luminosity samples, but is resolved with only one galaxy in the volume limited sample with the highest luminosity cut. Besides that, we see that there is a direct proportion between stellar mass and richness of groups. The same behaviour is observed in the lower panels that show the richness as a function of halo mass.

### 4.4 Effects of varying the mass function

While it is true that our method does not require any parameter, there are a couple of assumptions that can affect the results of the group finding.

The first is the assumption of the validity of eq. 1 to compute the stellar masses of individual galaxies. We have already tested the performance of such an approximation (see section 4.1) through comparisons with the stellar mass function. From the agreement we observe between the expected and our estimated stellar mass function we assume

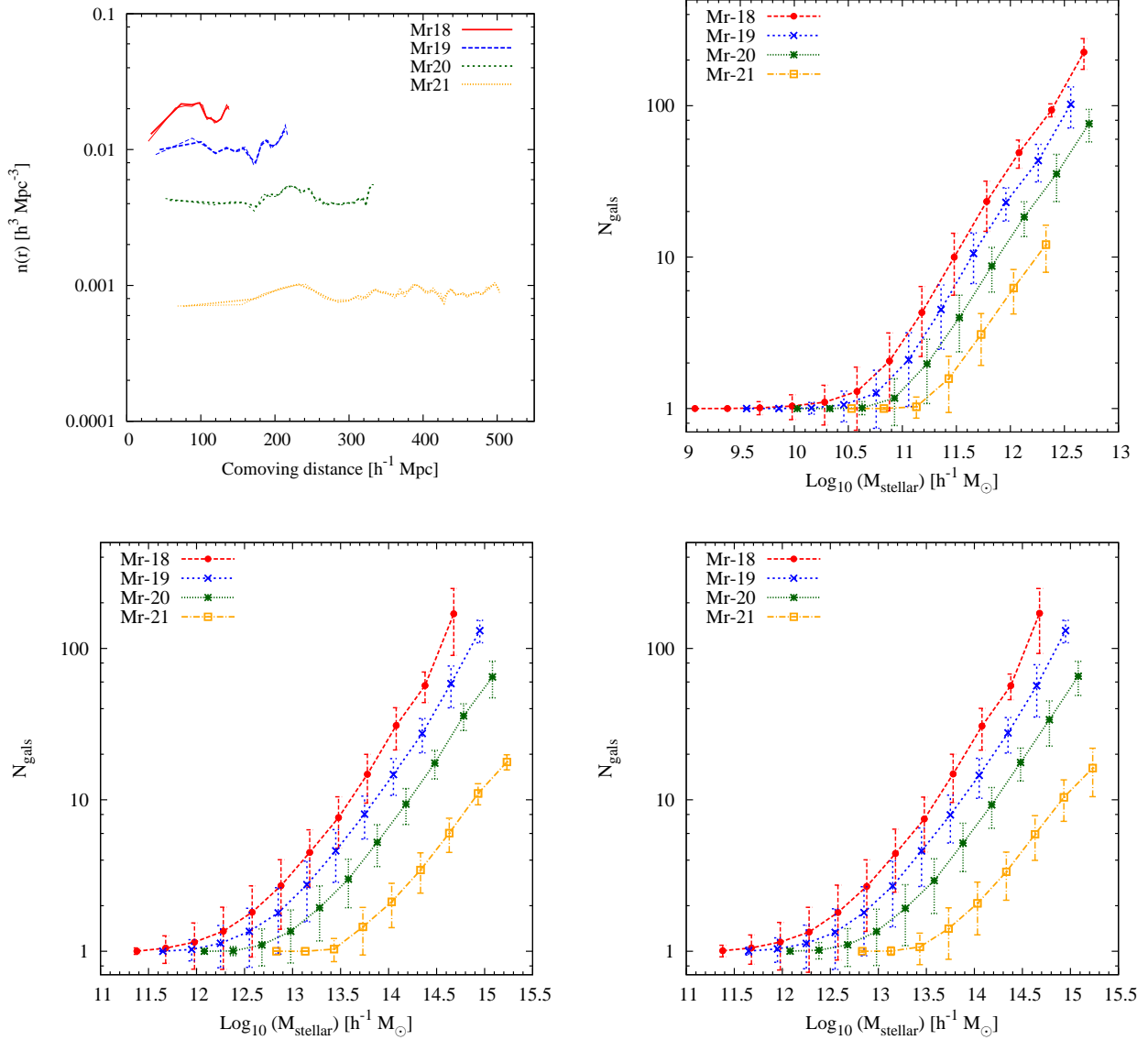


**Figure 8.** Mean number density of groups in the different samples as function of distance (upper left). Richness of groups as a function of group stellar mass (upper right), and halo mass estimated using the ranking of luminosities (lower left) and stellar masses (lower right). Solid lines show the mean value of the richness as a function of mass while the error bars indicate dispersion on the data in each bin.

there is no major influence on our results from this approximation.

The second assumption concerns the mass assignment. First, we assume that the halo virial mass is equivalent to the mass we draw from the halo mass function. It has been shown (White 2000) that there are deviations between our definition of virial mass and the halo mass estimated through different criteria (FoF mass, M200, etc.), but these deviations are not larger than a factor of two. This makes our mass estimates to be within the scatter of the mass distribution.

Finally, the shape of the assumed mass function can have an impact on the masses of the haloes associated to each group of galaxies. Since it is known that different fitting functions (Sheth & Tormen 2002, Warren et al. 2006, Reed et

al. 2007, Tinker et al. 2008) can give slightly different mass function, the procedure of reconstruction may be affected by this factor.

Figure 9 shows the final group stellar masses as a function of halo mass for groups of galaxies in two different volume limited samples, Mr-19 and Mr-21. In both cases the halo masses have been computed through the ranking of halo luminosities using the mass function from Sheth & Tormen (2002) and Warren et al. (2006). We can see that the halo masses assigned using the mass function of Warren et al. (2006) are systematically lower as compared with the samples of haloes with masses assigned from the Sheth-Tormen mass function. This differences should also affect the stellar masses, abundance of haloes and richness of groups, since the halo mass controls the virial radius and circular

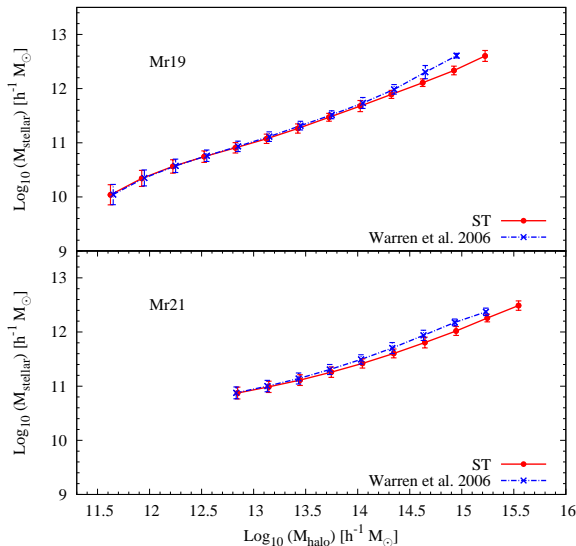


**Figure 9.** Median stellar mass as a function of halo mass for two of the samples, using two different mass functions, Sheth & Tormen (2002) and Warren et al. (2006). Halo masses are computed through the ranking of halo luminosities. Error bars indicate dispersion on the data in each bin.

velocity, which are used to compute the adaptive linking lengths of the search. This effect is stronger in the sample with the higher luminosity cut, and for high masses (larger than  $\sim 10^{13.5} h^{-1} M_{\odot}$ ) due to the fact that the differences between both mass functions are larger at the high mass end.

Because of the adaptive modifications in the linking lengths, the two halo catalogs are not identical, therefore we can not make a full one-to-one comparison between the masses assigned using the two mass functions.

However, we have seen that depending on the used mass function, one can have differences in the total number of groups by an order of 2%, slight changes in the stellar masses for haloes more massive than  $\sim 10^{11.5} h^{-1} M_{\odot}$  by in average  $\sim 0.1$  dex, and changes in the maximum halo mass by around 0.4dex. Despite these differences, which are observed mostly at the high mass end, the average statistical differences obtained using the different mass functions are small when one compares all the galaxy samples.

#### 4.5 Tests against mock catalogs

One of the best ways to test the performance of the group finder is using the results of semi-analytic methods of galaxy formation. For a galaxy catalog built from a semi-analytic method we can compare the results of our method against the original expected distribution of groups and galaxies and their properties.

To do this we have used the galaxy catalogs (De Lucia & Blaizot 2007, Croton et al. 2006) built from the millenium simulation (Springel et al. 2005). From the catalogs we have extracted a cubic subvolume of  $200h^{-1}$  Mpc side length. From this volume we built two samples using two different magnitude cuts in  $M_r$  of -18 and -19 to resemble our samples Mr-18 and Mr-19. Since the results are com-

parable for both samples, in the following we will present results only for the subsample with magnitude cut of -19.

For this sample we used the peculiar velocities of the galaxies to introduce redshift space distortions along the z-axis using the far observer approximation. We have run our group finder in two versions of the galaxy sample, one in real space and another in redshift space. Running the group finder for the set of galaxies in real space works as a control setup and allow us to identify the effects of the different approximations of the method in our results. Running the group finder in redshift space gives us information about the effect of redshift space distortions and contamination.

In Figure 10 we show the median halo mass - stellar mass relation for groups in the mock galaxy samples. Each line shows the relation for the original data from the mock catalog (Original), the groups identified in the sample using our group finder in real space (Real) and the groups identified with our method on the sample in redshift space (Redshift). In the figure, the thin-dashed line shows the scatter on the data for the sample in redshift space. One of the advantages of using mock catalogs is that it provides not only the information of the galaxy properties, but also provides the link to the properties of the host haloes. This allows us to check the reliability of the halo mass assignment. As it is shown in Figure 10, the halo mass assignment produces halo masses that show a very good agreement between the two samples and the original data. We can see that there are small deviations in the stellar-halo mass relation for the groups identified in both, real and redshift space. This is partly due to incompleteness in the galaxy and halo samples at low masses (similar to those discussed in Figure 4). As discussed in the previous section, another factor inducing small differences is the halo mass function used to perform the group finding, that might reproduce closely but not exactly the mass function of the simulation. We find that our method assigns a larger maximum mass to haloes in the high mass end. At the low mass end we have some low mass haloes in the true halo catalog which can not be regarded as individual haloes by our group finder and therefore are merged with other haloes.

Despite the small differences at the low and high mass ends, the median values of the stellar-halo mass relation show very good agreement, even for the sample in redshift space. The difference is well below the scatter of the data. A similar behaviour is observed in Figure 11 where we show the mean richness of haloes as a function of halo mass. Again the differences in the richness of haloes are smaller than the scatter in redshift space, where the method produces the largest scatter.

In order to provide a closer comparison, we have made a cross check of the halo masses for the groups of galaxies with the same central galaxy among the different samples. In Figure 12 we show the median one-to-one halo mass cross-check for the groups in the three samples. As it can be seen in the Figure, the one-to-one comparison shows very good agreement for the three samples, with the halo mass estimated from the group finder, in real as well as in redshift space, being slightly larger for haloes with masses above  $\sim 10^{13.5} h^{-1} M_{\odot}$ . From the figure it is evident that it is not an effect of the performance of the group finder in redshift space. The small difference of less than  $\sim 0.2$  dex between the original halo mass and the mass assigned by the group

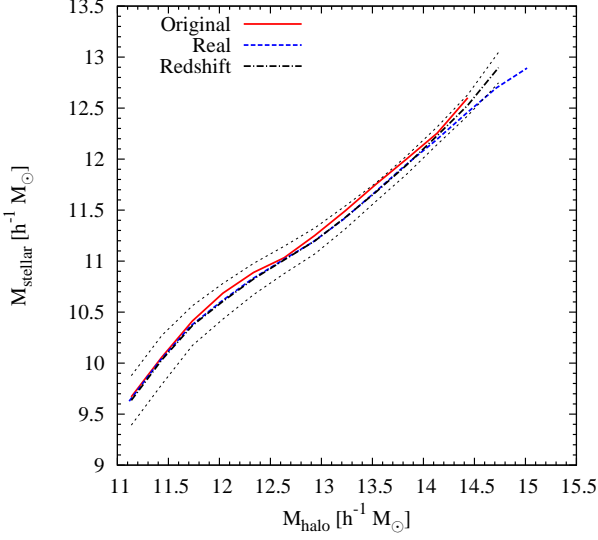


**Figure 10.** Median stellar mass - Halo mass relation for groups of galaxies in the mock catalog. The red solid line shows the values for original groups as obtained from the galaxy catalog. The blue dashed line show the groups identified using the group finder and the black dot-dashed line show the median value for the sample of galaxies in redshift space. The thin dashed line shows the scatter on the data for the sample of galaxies in redshift space.

finder comes mostly from the assumed mass function. As we have shown in Figure 9 it can influence the estimated halo mass especially at the high mass end. From these tests, we can conclude a good performance for the group finder. In particular we can see that the halo mass assignment produces very reliable results, with differences of the order of at most 0.2 dex. As expected, the richness of the groups is the most sensible quantity, and the effect is more noticeable at low halo mass, or equivalently for low richness groups, where we see that at a given halo mass the scatter increases, particularly for groups with richness below three. The good agreement we obtain between the two samples in real and redshift space with the original data from the simulation allows us to conclude that the approximations used in the method to estimate group-halo properties are reasonable, and that the scheme of group finding we propose produces reliable results. In general we see these results as a key point in favour of the quality and reliability of the method and its results.

A more direct check on the quality of the performance of the group finder and the quality of the group catalogs it produces is obtained through the analysis of the purity, completeness and contamination by interlopers in the groups identified from the mock catalog as introduced in Yang et al. (2007). Here we summarise the procedure and definitions.

Assume we have two group catalogs, one having the true groups, and the other one having the groups identified by the group finder in redshift space. We assume that two groups in the two catalogs are the same if the ID of the central galaxy is the same. The group in the true catalog has  $N_t$  galaxies, while the group identified by the group finder has  $N_f$  galaxies. If  $N_c$  represents the number of common galaxies

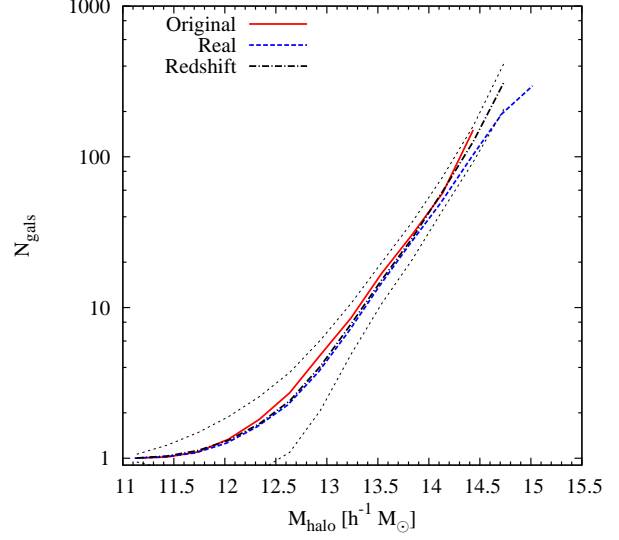


**Figure 11.** Mean richness of groups as a function of halo mass for the three samples, original, real space and redshift space. As in the previous figure, the thin lines show the scatter for the data of the sample of galaxies in redshift space.

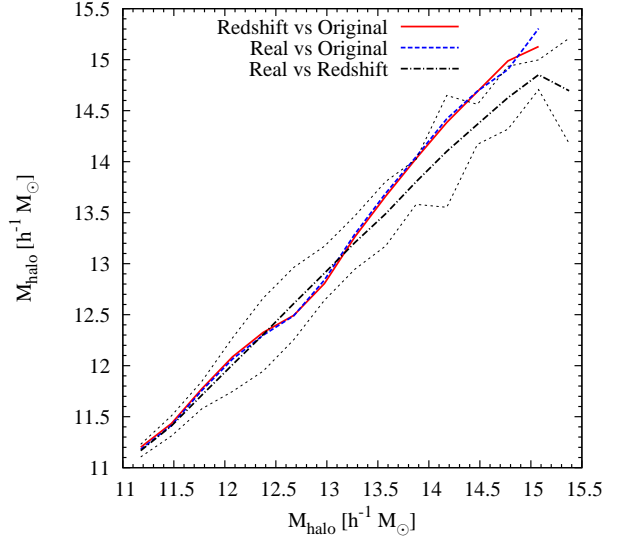


**Figure 12.** One to one comparison of the halo mass of haloes in the three samples. The solid red line shows the halo mass for the same haloes in the sample in redshift space against the halo mass in the original catalog. The blue dashed line shows the same for the groups in the sample in real space and the original catalog, and the black dot-dashed line shows the relation of the data in real and redshift space.

between the two groups, then we define the purity  $f_p$ , the completeness  $f_c$  and the contamination  $f_i$  as

$$\begin{aligned} f_p &\equiv N_t/N_f, \\ f_c &\equiv N_c/N_t, \\ f_i &\equiv (N_f - N_c)/N_t, \end{aligned} \quad (12)$$

Note that with this definition, a perfect group finder will produce groups with  $f_p = 1$ ,  $f_c = 1$  and  $f_i = 0$ .

In Figure 13 we show the distribution of values for the purity, contamination and completeness in percents. The solid line show the results for groups with at least one member, while the dashed line show the results for groups with at least two members. As mentioned in Yang et al. (2007), groups with only one member will have  $f_i = 0$ . To make a more precise analysis, it is necessary to account for the effect of the groups with only one member separately. Not including them hides the ability of the finder to identify real groups with only one member. Including them without considering (at least as a comparison) their effect on  $f_c$ ,  $f_i$  and  $f_p$  could lead to an overestimation of the quality of the group finder and the catalogs it produces, as it is shown in Figure 13.

In general, for groups with  $N_{\text{gals}} \leq 2$ , we see that around 64% of the groups have a purity of  $f_p = 1$ , 79% have purity between 0.7 and 1.3 and that around 94% of the groups have a purity between 0.5 and 1.5. On the other hand,  $\sim 80\%$  of the groups are hundred percent complete ( $f_c = 1$ ). 96% of all groups have completeness above 0.6 while  $\sim 87\%$  have completeness above 0.8. Finally, 73% of the groups have no contamination ( $f_i = 0$ ), while 92% of them have contamination lower than 0.5. In general these numbers indicate that the performance of the method is very good, and it is in average slightly better than the original method proposed in Yang et al. (2007). This good performance, and the parameter-free nature of the method are the most important features of the group finder.

## 5 SUMMARY AND DISCUSSION

We have presented a method for the identification of groups of galaxies and associated dark matter haloes in galaxy redshift surveys. We have applied the method to the data of the Seventh Data Release of the SDSS. The method, that works like a FoF method, uses a local and adaptive linking length that depends on the properties of haloes. The most important property of the method is that it does not depend on any parameter.

The method presented in this work is based on that introduced in Yang et al. (2007), nevertheless differs from it in several points. In our implementation of the method we do not need to make a first FoF procedure in redshift space to start the iterations of the groups. This avoids possible contamination by the choice of the initial linking lengths. Also, differently from the assumption made in Yang et al. (2007), we do not need to assume an initial value for the mass-to-light relation of groups. Finally, our method uses a two dimensional spheroid for the search of group members. This is different from the implementation in Yang et al. (2007), where they use a fixed FoF linking length for the transverse search and a probabilistic approach for the redshift distribution of galaxies, that at the end requires the use of another free parameter to fix the density contrast defining the membership of galaxies in groups.

We have shown that the stellar mass assignment for individual galaxies produces results that are in good agreement with the stellar mass function of Baldry et al. (2008). We also have seen that the stellar mass function of groups is

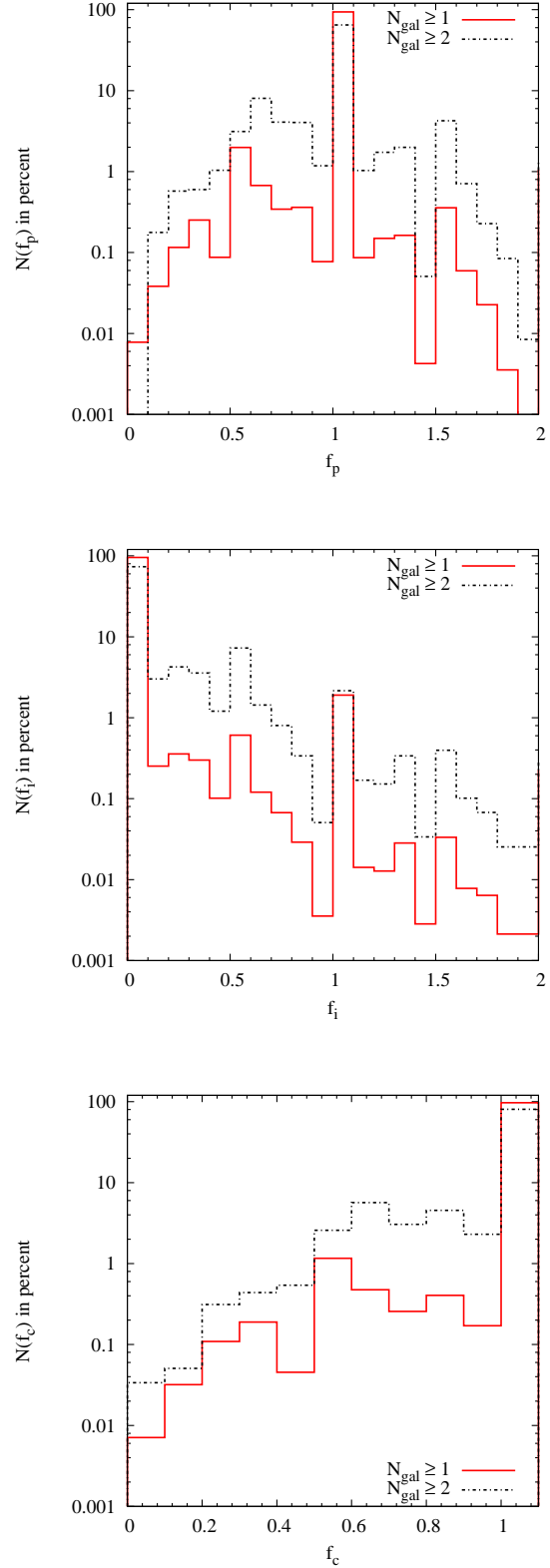


**Figure 13.** Distributions of purity (top), contamination by interlopers (middle) and completeness (bottom). The solid line shows the values for groups with at least two galaxies. As a comparison, the dashed line shows the values for groups with at least one galaxy.

more or less similar to the stellar mass function of individual galaxies for stellar masses smaller than  $\sim 10^{11.5} h^{-1} M_{\odot}$ . For stellar masses above  $10^{11.5} h^{-1} M_{\odot}$  the abundance of massive objects is larger for the groups than for the individual galaxies. This behaviour is expected, since groups of galaxies should have larger stellar masses than individual galaxies, increasing the abundance of stellar massive objects.

An important conclusion from the analysis of the stellar mass function of groups, that although trivial, is important to be quantified in detail. It concerns the effect of the richness of groups on their stellar content. We have seen in the stellar mass function for groups and also in the stellar-halo mass relation, that the stellar content of the volume limited sample built with the largest luminosity cut (Mr-21) has lower values for the group stellar masses. We have seen also that the richness of groups in this sample is the lowest one, due to the high luminosity cut that reduces the number density of galaxies in the sample. These results imply that most of the stellar content in groups of galaxies comes from objects with absolute magnitudes  $M_r$  larger than -19. This means that it is important to resolve the low luminosity component of groups of galaxies to acquire detailed information about their properties and specifically, its stellar content.

We have also shown that the groups built in this work follow the stellar-halo mass relation shown in Moster et al. (2010). We see that at halo masses larger than  $\sim 10^{13.5} h^{-1} M_{\odot}$  there is an increase in the stellar mass of our groups, making groups hosted in these massive haloes to have larger stellar mass content (larger than  $\sim 10^{11.5} h^{-1} M_{\odot}$ ) than expected from the prediction of Moster et al. (2010). We have shown that this deviation vanishes when the stellar-halo mass is plotted using only the stellar mass of the central galaxy in each group. Therefore the large abundance of high stellar mass groups is due to the contribution of satellite galaxies in rich groups.

We have also shown that the halo mass computed from the ranking of the group luminosities  $M_{h,L_{ch}}$  or from the ranking of the stellar mass  $M_{h,M_s}$  are in good agreement. Furthermore, as a confirmation of the robustness of the mass assignment, we see that the halo mass assignment produces results that are in agreement among all our four samples.

Tests against galaxy catalogs from semi-analytic methods have proven the good performance of the method, showing that we can recover with high precision the properties of the groups of galaxies and haloes in the catalog. Specifically, a one-to-one comparison has shown that the halo masses are in good agreement, but are slightly off by at most 0.2 dex for halo masses larger than  $10^{13.5} h^{-1} M_{\odot}$ . On the other hand, purity, completeness and contamination indicators show a good performance of the method, and in general, show to be better than the ones presented by Yang et al. (2007). The validation of the method with galaxy catalogs provides us with strong evidence in favour of the convenience of the use of this method for the identification of galaxy groups residing in the same dark matter halo.

We have found that the only possible factor that can influence the final results of our group-halo identification is the selection of the mass function. To test the influence of this factor on our results, we have compared the results of the identification of groups in two of the samples. For them we have computed the halo masses from two different mass functions. We have seen that depending on the used

mass function one can have differences in the total number of groups of about 2%. We observe a slightly changes in the stellar masses of groups (in average on  $\sim 0.1$  dex) hosted in haloes more massive that  $\sim 10^{14.5} h^{-1} M_{\odot}$ . We see also changes in the maximum halo masses of around  $\sim 0.4$  dex. Despite these differences, that are observed only at the very high halo masses, overall differences obtained using different mass functions are minor.

Finally we have shown the richness of our groups as a function of different group-halo properties. First we have seen that we can recover a constant mean number density of groups in space, as it should be the case for volume limited samples. We have seen that indeed the volume limited nature of the samples affects the richness of the groups at a given halo property, groups in samples with a high luminosity cut are naturally less rich. This has an important effect in the estimation of the stellar mass of groups but does not have implications on the halo mass assignment, and therefore in the procedure of group identification.

## ACKNOWLEDGMENTS

J.C.M. wants to give thanks to German Science Foundation (grant MU 1020/6-4). The authors wants to thanks Sebastian Nuza for his useful comments on the manuscript. The Millennium Simulation databases used in this paper and the web application providing online access to them were constructed as part of the activities of the German Astrophysical Virtual Observatory. Funding for the Sloan Digital Sky Survey (SDSS) has been provided by the Alfred P. Sloan Foundation, the Participating Institutions, the National Aeronautics and Space Administration, the National Science Foundation, the U.S. Department of Energy, the Japanese Monbukagakusho, and the Max Planck Society. The SDSS Web site is <http://www.sdss.org/>. The SDSS is managed by the Astrophysical Research Consortium (ARC) for the Participating Institutions. The Participating Institutions are The University of Chicago, Fermilab, the Institute for Advanced Study, the Japan Participation Group, The Johns Hopkins University, Los Alamos National Laboratory, the Max-Planck-Institute for Astronomy (MPIA), the Max-Planck-Institute for Astrophysics (MPA), New Mexico State University, University of Pittsburgh, Princeton University, the United States Naval Observatory, and the University of Washington.

## REFERENCES

- Abazajian, K. N., Adelman-McCarthy, J. K., Agüeros, M. A., et al. 2009, *ApJS*, 182, 543
- Baldry, I. K., Glazebrook, K., & Driver, S. P. 2008, *MNRAS*, 388, 945
- Berlind, A. A., Frieman, J., Weinberg, D. H., et al. 2006, *ApJS*, 167, 1
- Blanton, M. R., Hogg, D. W., Bahcall, N. A., et al. 2003, *ApJ*, 592, 819
- Blanton, M. R., Schlegel, D. J., Strauss, M. A., et al. 2005, *AJ*, 129, 2562
- Blanton, M. R., & Roweis, S. 2007, *AJ*, 133, 734
- Bryan, G. L., & Norman, M. L. 1998, *ApJ*, 495, 80

- Crook, A. C., Huchra, J. P., Martimbeau, N., et al. 2007, *ApJ*, 655, 790
- Croton, D. J., Springel, V., White, S. D. M., et al. 2006, *MNRAS*, 365, 11
- De Lucia, G., & Blaizot, J. 2007, *MNRAS*, 375, 2
- Koester, B. P., McKay, T. A., Annis, J., et al. 2007, *ApJ*, 660, 239
- Lee, B. C., Allam, S. S., Tucker, D. L., et al. 2004, *AJ*, 127, 1811
- Merchán, M. E., & Zandivarez, A. 2005, *ApJ*, 630, 759
- Moster, B. P., Somerville, R. S., Maulbetsch, C., et al. 2010, *ApJ*, 710, 903
- Muñoz-Cuartas, J. C., Müller, V., & Forero-Romero, J. E. 2011, *MNRAS*, 417, 1303
- Nichol, R. C. 2004, *Clusters of Galaxies: Probes of Cosmological Structure and Galaxy Evolution*, 24
- Reed, D. S., Bower, R., Frenk, C. S., Jenkins, A., & Theuns, T. 2007, *MNRAS*, 374, 2
- Sheth, R. K., & Tormen, G. 2002, *MNRAS*, 329, 61
- Springel, V., White, S. D. M., Jenkins, A., et al. 2005, *Nature*, 435, 629
- Tago, E., Einasto, J., Saar, E., et al. 2008, *A&A*, 479, 927
- Tago, E., Saar, E., Tempel, E., et al. 2010, *A&A*, 514, A102
- Tinker, J., Kravtsov, A. V., Klypin, A., et al. 2008, *ApJ*, 688, 709
- Tinker, J., Wetzel, A., & Conroy, C. 2011, *arXiv:1107.5046*
- Wang, Y., Yang, X., Mo, H. J., et al. 2008, *ApJ*, 687, 919
- Wang, H., Mo, H. J., Jing, Y. P., Yang, X., & Wang, Y. 2011, *MNRAS*, 413, 1973
- Warren, M. S., Abazajian, K., Holz, D. E., & Teodoro, L. 2006, *ApJ*, 646, 881
- Weinmann, S. M., Lisker, T., Guo, Q., Meyer, H. T., & Janz, J. 2011, *MNRAS*, 416, 1197
- Wen, Z. L., Han, J. L., & Liu, F. S. 2009, *ApJS*, 183, 197
- Wetzel, A. R., Tinker, J. L., & Conroy, C. 2011, *arXiv:1107.5311*
- Yang, X., Mo, H. J., van den Bosch, F. C., et al. 2007, *ApJ*, 671, 153
- Zandivarez, A., & Martínez, H. J. 2011, *MNRAS*, 415, 2553
- Zapata, T., Perez, J., Padilla, N., & Tissera, P. 2009, *MNRAS*, 394, 2229

This paper has been typeset from a  $\mathrm{T}_{\mathrm{E}}\mathrm{X}$ / $\mathrm{L}^{\mathrm{A}}\mathrm{T}_{\mathrm{E}}\mathrm{X}$  file prepared by the author.